Journal of the Serbian Chemical Society
JSCS-info@shd.org.rs • www.shd.org.rs/JSCS
J. Serb. Chem. Soc. 82 (3) 329–342 (2017)
JSCS–4969
UDC 666.122.5.000.57:544.351:544.27
Original scientific paper

Dissolution behavior of a polyphosphate glass in simulated body fluid

JELENA D. NIKOLIĆ[1]*, MIHAJLO B. TOŠIĆ[1], SNEŽANA R. GRUJIĆ[2], VLADIMIR D. ŽIVANOVIĆ[1], MARIJA S. ĐOŠIĆ[1], SRĐAN D. MATIJAŠEVIĆ[1] and SONJA V. SMILJANIĆ[2]

[1]*Institute for Technology of Nuclear and other Mineral Raw Materials, 86 Franchet d'Esperey St., 11000 Belgrade, Serbia and* [2]*Faculty of Technology and Metallurgy, University of Belgrade, Karnegijeva 4, 11000 Belgrade, Serbia*

(Received 31 October, revised 5 December, accepted 6 December 2016)

Abstract: In this work, the dissolution behavior of a polyphosphate glass, with the composition $45P_2O_5 \cdot 3SiO_2 \cdot 25K_2O \cdot 15CaO \cdot 10MgO \cdot ZnO \cdot MnO$ (mol %), in simulated body fluid (SBF) at a temperature of 37 °C for different times was studied. Two powder sizes of the glass (granulation: 0.1–0.3 and 0.3–0.65 mm) and the bulk glass were investigated. The dissolution experiments were conducted under stationary conditions. Changes in the normalized mass release, normalized concentration of ions, pH values, and surface morphology were determined as a function of the dissolution time. The initial rates of glass powder dissolution and leaching of ions, as well as the diffusion coefficient of cations and the releasing rate of ions, during the hydrolysis process of glass were determined. It was shown that the investigated phosphate glass dissolves in SBF incongruently, with neither precipitation nor the formation of newly potentially toxic compounds, in a dissolution period 720 h.

Keywords: biophosphate glass; leaching; kinetics; mechanism.

INTRODUCTION

Within the group of biomaterials that could be used as an implant in a living organism, bioglasses have received great attention.[1] Resorbable biomaterials could significantly shorten the time necessary for restorations of functional loading of grafted bones.[2] Phosphate-based glasses, known as biodegradable and resorbable biomaterials, could be used for bone replacement. Depending on the composition, the degradation rates of phosphate glasses in a physiological environment could be varied from hours to several weeks.[3,4] The dissolution rates of glasses affect the proliferation of osteoblast-like cells.[5] Moreover, changing the solubility of glasses through the glass composition influences the cell response.[6]

* Corresponding author. E-mail: j.nikolic@itnms.ac.rs
doi: 10.2298/JSC161031009N

It is known that the presence of metal cations in the human body is demanded for its proper functioning. These ions induce specifically biological effects, *e.g.*, from enhancing osteoblast activity to influencing antibacterial properties.[4,7–9] One of the advantages of bioglass application is the possibility to include the desired metal cations in the bioglass structure during the synthesis process. In this way, a bioglass could serve as a source of many of the essential elements that improve bone growth, such as Zn, Cu, F, Mn, Sr, Mg and B.[10,11] Furthermore, another advantages of bioglass application is the possibility of controlled ions release, thus offering the opportunity of a wide range for bone regeneration therapy.[12,13] The success of biomaterial interaction with tissue depends on both the properties of implanted material and of the condition of the host tissue.[13] Degradation of phosphate glasses *in vivo*, as resorbable biomaterials, occurs through non-toxic products, which are eliminated from the body.[1]

In this study, the dissolution properties of polyphosphate glass with a mole ratio of $(M_2O + MO)/P_2O_5 > 1$ in simulated body fluid (SBF) at 37 °C were investigated (M being the modifying cations). Static dissolution tests were conducted with powdered glass and bulk glass samples. The mechanisms and kinetics of the dissolution process were analyzed and are discussed.

EXPERIMENTAL

Glass preparation

The composition of the studied glass was derived from the basic P_2O_5–K_2O–CaO system. The content of the main network glass forming oxide, P_2O_5, was 45 mol %. With the aim of controlling the dissolution characteristics and crystallization ability of the glass, 3 mol % of SiO_2 was added. The content of K_2O was fixed at 25 mol %. Divalent cation oxides, such as Ca^{2+}, Mg^{2+}, Zn^{2+} and Mn^{2+}, were added in order to obtain 100 mol % of the glass.

Appropriate glass batch compositions were prepared using reagent grade raw materials $(NH_4)_2HPO_4$ (*p.a.* grade, Sigma–Aldrich), K_2CO_3 (*p.a.* grade, Analytika Ltd.), $CaCO_3$ (*p.a.* grade, Carlo Erba), SiO_2 (*p.a.* grade, Lachner), MgO (*p.a.* grade, Eurohemija), ZnO (*p.a.* grade, Kemika) and MnO_2 (*p.a.* grade, Merck). The raw materials were dried at 105 °C for 3 h, then, they were weighed and mixed in an agate mortar to obtain a homogeneous glass mixture.

Glass melting was performed at 1230 °C during 1 h in an electrical furnace (CARBOLITE BLF 17/3) using an open unglazed porcelain crucible. Then, the glass melt was subjected to quenching on a steel plate. By visual analysis, the obtained glass was homogeneous, colorless and transparent.

In order to investigate the dissolution behavior of the prepared glass, two sets of dissolution experiments were performed: two classes of powders and bulk glass.

Dissolution experiments

The glass powder was prepared by crushing the bulk glass in an agate mortar and sieving to an appropriate grain size. After sieving, the glass particles were separated into two classes with respect to the particle size: 0.1–0.3 mm and 0.3–0.65 mm.

After the separation, both classes of the glass powder were rinsed six times, each time with 30 mL of distilled water, in order to remove glass dust. Afterwards, the glass powders were dried to constant mass at 105 °C for 3 h and then used for further analysis.

The SBF solution was prepared according to recommendations[14] by dissolving the reagent-grade chemicals of NaCl (Sigma–Aldrich 99.99 %), $NaHCO_3$ (Sigma–Aldrich BioXtra), KCl (Merck ≥ 99.99 %), $K_2HPO_4 \cdot 3H_2O$ (Sigma–Aldrich for molecular biology), $MgCl_2 \cdot 6H_2O$ (Sigma–Aldrich BioXtra), 1.0 mol dm^{-3} HCl (Merck), $CaCl_2$ (Merck ≥ 99.99 %), Na_2SO_4 (Merck ≥ 99.99 %) and tris(hydroxymethyl)aminomethane, $(CH_2OH)_3CNH_2$, Sigma–Aldrich 99.99 %) in distilled water.

Dissolution experiments, conducted under stationary conditions, consisted in weighing 1.0 g of glass powder, placing it into volumetric flasks and adding 50 mL of SBF. The volumetric flasks with glass powders and SBF were placed in a Haake water bath with digital control (sensitivity of ±0.1 °C), previously set to a temperature of 37 °C and kept there for different times, from 0.5 to 720 h.

After the scheduled time, the flask content was filtered and glass powder was separated from the colorless solutions. The pH and concentration of ions in the obtained leachate were determined. The filter papers were weighted before the experiment. The filter papers with the glass powders, obtained for all the different dissolution times, were dried to constant mass at 105 °C and then weighed to determine the mass release during the dissolution in SBF.

The two powdered classes were subjected to AAS, UV/Vis and pH analyses to monitor the mass loss, ion concentration and pH values after the dissolution experiments. SEM, FTIR, and XRD analyses were realized using the bulk glass of dimension 1.0 cm×1.0 cm×0.5 cm. Namely, the samples of bulk glass were crushed after the dissolution experiments to prepare for the FTIR and XRD analyses.

Analytical methods

Atomic absorption and UV/VIS spectroscopy. Concentrations of the ions in filtrate after dissolution were determined using a Perkin Elmer 703 atomic absorption spectrometer and a Philips UV/Vis 8610 spectrophotometer.

pH Measurements. A Consort C830P pH meter was used for the pH measurements of the filtrates after the dissolution experiments of the glass powders in SBF. The measurements were conducting at 25 °C. The pH measurements were with errors in the range 0.02–0.16.

FTIR Analyses. Fourier transform infrared (FTIR) spectroscopy was realized using an MB Bomen Hartmann FTIR spectrometer in the wave number range 4000–400 cm^{-1}. The FTIR analyses were performed on bulk glass in untreated form and after the dissolution experiments. The samples were prepared for FTIR analysis by crushing. The FTIR vibration spectra were recorded at room temperature using the KBr pellet technique.

SEM Analyses. Bulk glass samples previously immersed in SBF for 48, 96, 120 and 240 h were prepared by sputtering with gold in a Leica SCD005 device and investigated by SEM (Jeol JSM-6610LV) in order to evaluate the surface microstructure. The SEM was operated simultaneously in the secondary electron mode (SEI) and the backscattered electron mode (BES). Compositional analysis was performed by energy dispersive spectroscopy (EDS, Max large area analytical silicon drift) connected to an INCA Energy 350 microanalysis system.

Density and specific surface area. The density of glass was determined by the Archimedes method. The specific surface areas (s) of the glass powders were determined by the laser diffraction (LD) method using a Fritsch Analysette 22 laser particle sizer.

RESULTS AND DISCUSSION

Based on the chemical analysis, the nominal and analyzed compositions of the glass are given in Table I. According to the results, the composition of

obtained glass closely corresponded to the selected composition, within the range of experimental error.

TABLE I. Composition of the glass, mol %

Composition	P_2O_5	SiO_2	K_2O	CaO	MgO	ZnO	MnO
Nominal	45	3	25	15	10	1	1
Analyzed	45.4	3.1	25.6	14.5	9.3	1.2	0.9

The glass investigated in this study belongs to the polyphosphate types. Polyphosphate glasses consist of phosphate chains that contain Q^2 tetrahedra (two bridging oxygen atoms) and a terminal Q^1 tetrahedra (one bridging oxygen atom). The density of the glass was 2.705 g cm^{-3}. The specific surface area (s) of the glass powder sample with granulation ranging from 0.1 to 0.3 mm was 0.0367 m^2 g^{-1}, while it was 0.0178 m^2 $g^{-1}$for the powder sample with granulation ranging from 0.3 to 0.65 mm,.

Dependence of normalized mass release and normalized ion concentration on dissolution time

Normalized mass release, f_m (g m^{-2}), was calculated using the experimental values of mass release and the specific surface areas (s) of the powders. The dependences of the normalized mass release of the glass powders for two different granulations on the dissolution time in SBF are shown in Fig. 1.

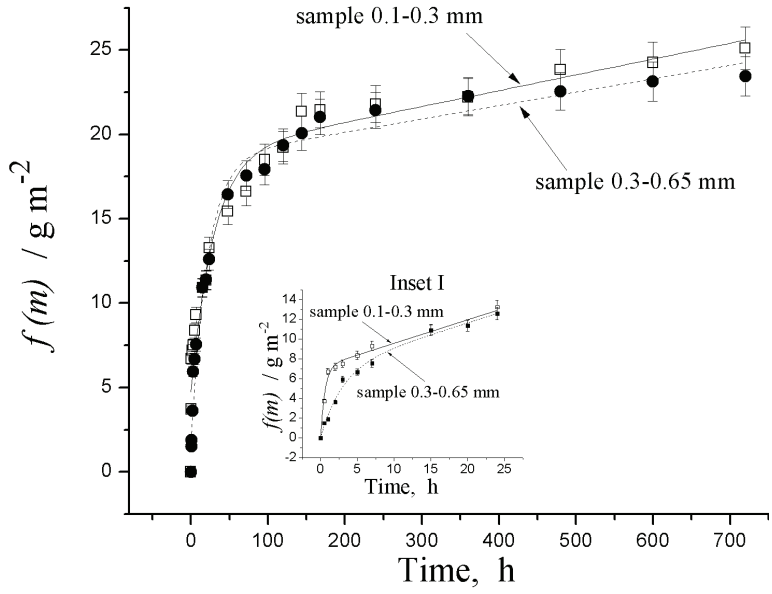

Fig. 1. Dependence of the normalized mass release on the dissolution time in SBF at 37 °C.

For shorter dissolution times (Fig. 1, inset I), the differences between f_m for both classes were higher, compared to the values for the longer dissolution times (> 240 h) where the differences were smaller.

To compare the release of different leached species as an appropriate parameter, the normalized *i*-th element mass release from unit area (f_i) was used:[15–20]

$$f_i = \frac{c_i V}{\delta_i S} \tag{1}$$

where c_i is the mass concentration of the leached species in time t, δ_i is the mass fraction of species i in the glass, S is the glass surface in contact with the solution, and V is the solution volume.

Based on the experimentally measured ion concentrations, the normalized ion concentrations in the solution, f_i, were calculated using Eq. (1). The dependences of the normalized concentrations of the ions on the dissolution time for both studied classes are presented in Fig. 2. The differences between the values for the normalized concentrations of the ions with respect to the granulation of the starting glass powder were quite small (Fig. 2). For shorter dissolution times, up to 20 h, the values of the normalized concentrations of the ions showed the largest changes with respect to the granulation of the samples. This so-called "initial stage" of dissolution might be described as a linear dependence of normalized concentrations of the ions on dissolution time. At this stage, the highest rate of dissolution could be observed. Additionally, this stage had the shortest duration.

For dissolution times from 20 to 240 h, the "initial stage" of dissolution was followed by a "transitional stage". The trend in the changes in the values of the normalized concentrations of the ions indicates a significant decrease in the dissolution rate of glass in the "transitional stage". In the third stage, for dissolution times from 240 to 720 h, named the "final stage", a linear dependence of the normalized concentrations of ions was observed, but the changes during the dissolution were quite small. The glass dissolution rate in this stage was several orders of magnitude lower than the initial dissolution rate.

The time-dependent values of the pH of the solution are presented in Fig. 3. For both granulations, the same trend in the changes of the pH values could be observed. The breakage of P–O–P bonds led to the release of H^+, causing a decrease in the solution pH values.[21,22] For shorter dissolution times, the pH values decreases faster for the sample with granulation in the 0.1–0.3 mm range. The difference between the pH values for the same dissolution times as a function of time was higher in the "initial stage", while the differences were quite small in the "final stage".

The SEM micrographs of the surfaces of the glass bulk after dissolution in SBF for 48, 96, 120, and 240 h are shown in Fig. 4.

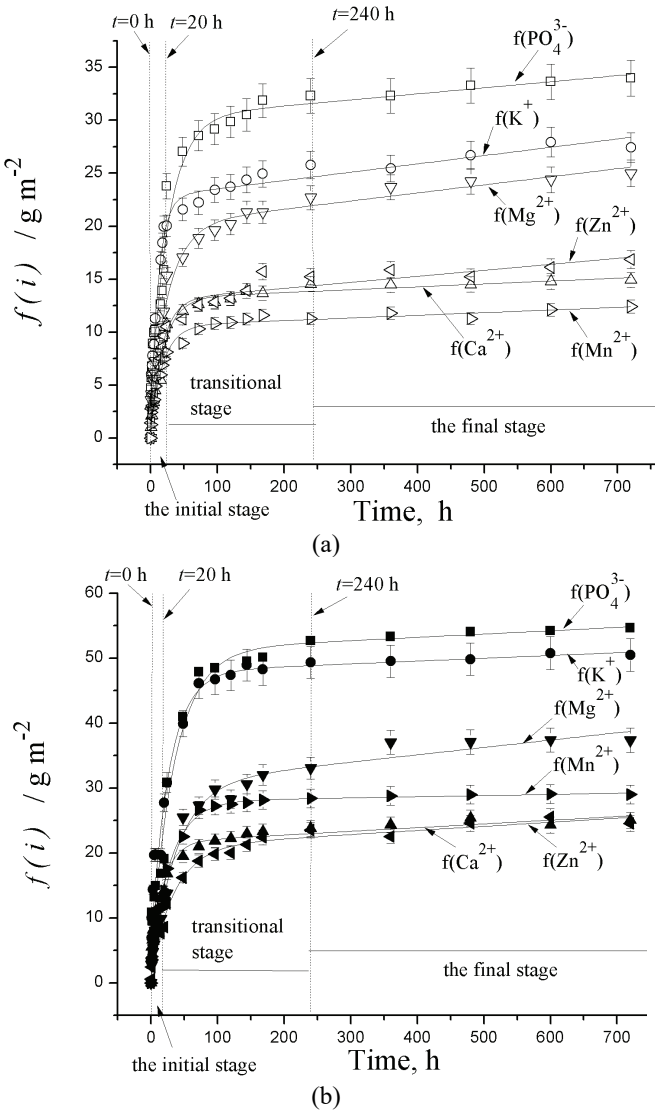

Fig. 2. Dependence of the normalized concentration of ions on the dissolution time in SBF at 37 °C for two studied classes of the glass: a) 0.1–0.3 and b) 0.3–0.65 mm.

Figure 4a indicates the formation of pits and a honeycomb-like structure at the beginning of the dissolution process. On prolonging the treatment, the honeycomb-like structure covered all the surface of the glass. After 96 h of dissolution, a white layer on the surface could be observed (Fig. 4b). The white layer was porous, fragile and could be detached easily from the rest of the compact glass sample. For longer dissolution times, the grain structure of the white layer with

many cavities could be noticed (Fig. 4c). The white layer and the native glass below the white layer are clearly visible in Fig. 4d). The thickness of the white layer after a dissolution time of 120 h was in the range 0.9–1.1 μm, while after 240 h of dissolution, the thickness was in the range 1.2–1.7 μm.

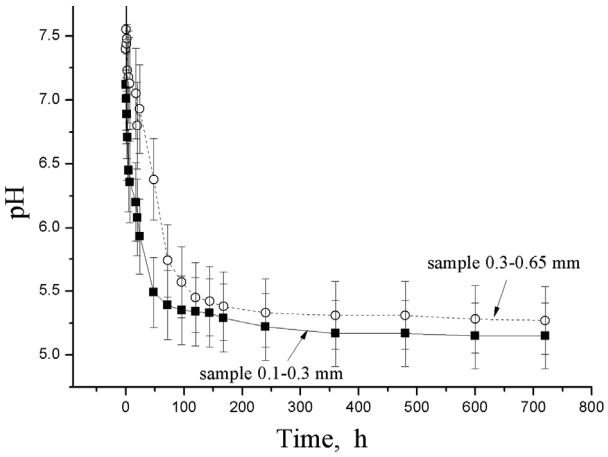

Fig. 3. Time-dependence values of the pH solution during the dissolution experiments.

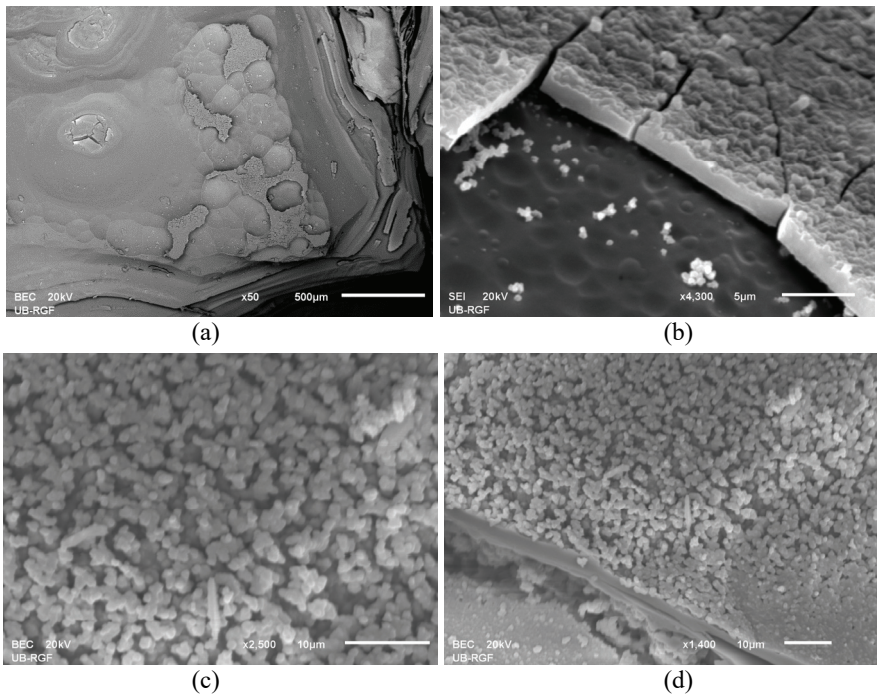

Fig. 4. SEM micrographs of the glass bulk surfaces after dissolution in SBF for a) 48 h, b) 96 h, c) 120 h and d) 240 h.

The results of EDS analysis (not shown) realized at the bulk glass surface (untreated and after dissolution). The intensities of the peaks arising from the different elements were changed. Namely, the intensity of the peaks decreased significantly with dissolution time, indicating decreases in their concentration in the surface layer.

The XRD patterns of an untreated glass sample (a) and one immersed in SBF for 240 h (b) are shown in Fig. 5. The shapes of the diffractograms for an untreated glass sample as well as for one immersed in SBF are almost the same. Namely, the immersed sample did not show the presence of any new crystalline phase at its surface. This result shows that SBF dissolves the sample without the formation of crystalline phases.

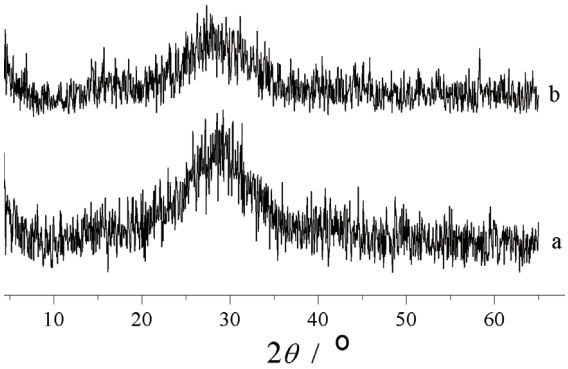

Fig. 5. XRD of a) an untreated glass sample and b) a glass sample immersed in SBF for 240 h.

The FTIR spectra of the untreated glass sample and samples that had been immersed in SBF for 48 , 96 and 120 h are shown in Fig. 6. The FTIR spectrum of the untreated glass sample is presented in Fig. 6a, from which it could be seen that dominant absorption peaks are visible at 1350, 1220, 1060, 950, 810 and 660 cm^{-1}. The peaks at 1350 and 1220 cm^{-1} could be attributed to the asymmetric and symmetric stretching motion of the two non-bridging oxygen atoms bonded to a phosphorus atom, the $(PO_2)^-$ groups (characteristic of Q^2 tetrahedra).[23,24] The peaks at 1060 and 950 cm^{-1} may appear due to the asymmetric and symmetric stretching motion of a non-bridging oxygen atom bonded to a phosphorus atom in the Q^1 tetrahedra.[25,26] The peak at 810 cm^{-1} is assigned to the motions of bridging oxygen atom (P–O–P) in the Q^1 tetrahedra, while the peak at 660 cm^{-1} corresponds to the symmetric stretching motion of bridging oxygen atom (P–O–P) in the Q^2 tetrahedra. The FTIR spectra of the samples treated in SBF indicate the disappearance of peaks characteristic for the Q^2 tetrahedra present in polyphosphate chains. Furthermore, broadenings are visible in the area between 1020 and 660 cm^{-1}, which correspond to the presence of pyro- and orthophosphate groups formed by the destruction of the polyphosphate chains during the glass hydrolysis process. This confirms the occurrence of glass network depolymerization.

Using the experimentally determined dependencies of the normalized mass release and the normalized ion concentrations (Figs. 1 and 2) on dissolution time, the starting dissolution rates of the species ($r_{0,i}$) were calculated from the slopes of linear part of the curves in the initial stage of the dissolution for both samples. The results are presented in Table II.

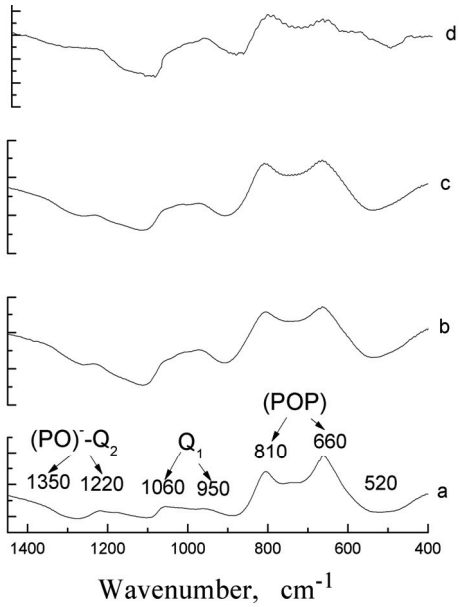

Fig. 6. FTIR spectra of a) untreated glass sample; b), c) and d) glass samples that had been immersed in SBF for 48, 96 and 120 h, respectively.

TABLE II. Initial ion release rates, $r_{0,i}$ / g m^{-2} h^{-1}

Granulation mm	Rate						
	$r_{0,m}$	$r_{0,PO_4^{3-}}$	r_{0,K^+}	$r_{0,Ca^{2+}}$	$r_{0,Mg^{2+}}$	$r_{0,Zn^{2+}}$	$r_{0,Mn^{2+}}$
0.1–0.3	0.53	0.57	0.84	0.40	0.44	0.42	0.32
0.3–0.65	0.52	0.56	0.75	0.47	0.35	0.38	0.39

As could be seen, the initial dissolution rates have similar values for $r_{0,m}$ and $r_{0,PO_4^{3-}}$, while r_{0,K^+} has the highest value. The similar values for $r_{0,m}$ and $r_{0,PO_4^{3-}}$ show that the phosphorus was released by the dissolution of the glass matrix, *i.e.*, by hydrolysis of the glass network. Moreover, it is obvious that the initial dissolution rates were higher for all ions, except Ca^{2+} and Mn^{2+}, and for the class having a granulation fraction of 0.1 to 0.3 mm. This shows that the sample surface had a great impact on the starting dissolution rate of ions in SBF.

The ion exchange reactions that occurred simultaneously with hydrolysis of the covalent bonds of the glass network were identified[15,16,27] as key processes of glass dissolution. In the initial stage, interdiffusion and exchange of the cations in the glass with protons from the solution were dominant. In the final stage, the

process of hydrolysis of the covalent bonds of the glass network was predominant. Therefore, with the aim of characterizing the dissolution process, following parameters should be known: a) the effective diffusion coefficients of ions (D_i) and b) the release rates by hydrolysis (r_{hi}). These parameters were determined by treatment of the experimental results.

Time dependence of normalized leached masses of ions, f_i, in the initial stage can be describe by relation:[15]

$$f(i) = \rho\sqrt{\frac{D_i t}{\pi}} \tag{2}$$

where ρ is the glass density and t is time. The diffusion coefficients of the cations were calculated using Eq. (2), based on concentrations determined after 5 h exposure to SBF.

The results of the calculated diffusion coefficients of cations in both classes of samples are presented in Table III. By comparing the results of the calculations, it is evident that similar values were obtained for each cation, regardless the granulation of the sample. According to the literature, the diffusion coefficients values calculated in this study are similar to those reported in the literature.[28,29]

TABLE III. Values of cations diffusion coefficients, $D(i)\times10^{13}$ / m^2 h^{-1}, for the dissolution of the samples

Granulation mm	Coefficient				
	$D(K^+)$	$D(Ca^{2+})$	$D(Mg^{2+})$	$D(Zn^{2+})$	$D(Mn^{2+})$
0.1–0.3	1.90	0.215	1.33	0.917	0.776
0.3–0.65	2.94	1.63	1.26	1.05	1.28

The main characteristic of the transitional stage in the dissolution process was the rapid decrease in the dissolution rate of the glasses. Such a change in the dissolution rate is mainly associated with the formation of a hydrated layer of glass, increasing the concentration of elements from the glass in the solution and reducing the dissolution rate due to the influence of chemical affinity and surface passivation of the glass.[30] Based on the experimental results, the change in the release rate of ions at this stage could be displayed using the correlation:[31]

$$r_i(t) = \frac{f_i(t) - f_i(t - \Delta t)}{\Delta t} \tag{3}$$

where Δt is the time interval between two sequential experimental times.

The dependence of the dissolution rate on time is shown in Fig. 7 for both granulation fractions. For all dissolution times, compared to the initial dissolution rate, an exponential decrease in the dissolution rate with time could be observed.

The dissolution rates of the ions were 12 to 15 times smaller than the initial dissolution rate, while the rate of glass powder dissolution was about 11 times smaller with respect to the initial dissolution rate. However, at times to 720 h, the differences in the values of the dissolution rate of ions were small, but still existed. This indicated that the mechanism of glass dissolution was congruent**.** Since the experiments were performed under static conditions (without changing the volume of the solution), the reasons the reduction of the dissolution rate of ions may be primarily a consequence of an increase in the concentration of dissolved ions. Increased concentrations of elements in the solution, previously dissolved from the glass, affect a change in the chemical affinity of the solution for the glass, causing a reduction in the release rate of ions from the glass into the solution.

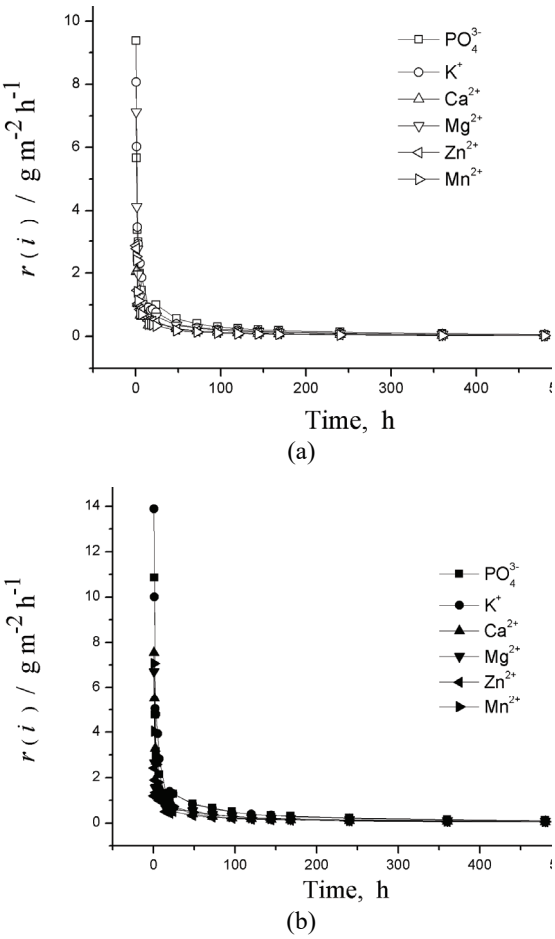

Fig. 7. Dependence of the dissolution rate of ions, (r_i), on time at 37 °C for two classes: a) 0.1–0.3 mm and b) 0.3–0.65 mm.

After the period of exponential decrease, the final stage was characterized by a slow decrease in the dissolution rate, denoted as “remaining” or “final” dis-

solution rate. Hydrolysis of the glass network is the dominant mechanism at the final stage of dissolution. This stage could be observed as a region with a linear dependence of the changes in the ion concentration with time (Fig. 2). The slopes of the linear part of the curves in the final stage of dissolution determine the release rates r_{hi} by hydrolysis.[30,31]

By calculating the slope of the linear part of the curves (Fig. 2) after 240 h of dissolution, the dissolution rates of the ions, r_{hi}, were determined in the final stage for both glass sizes. The results are presented in Table IV.

TABLE IV. The ions dissolution rates, $r_{hi}\times10^3$ / g m^{-2} h^{-1}, in the final stage

Granulation mm	Rate					
	$r_h(PO_4^{3-})$	$r_h(K^+)$	$r_h(Ca^{2+})$	$r_h(Mg^{2+})$	$r_h(Zn^{2+})$	$r_h(Mn^{2+})$
0.1–0.3	3.90	4.81	0.874	4.44	4.95	2.16
0.3–0.65	4.03	2.95	2.05x	7.44	4.19	1.28

Comparing the results of both studied classes, it could be concluded that granulation had no significant effect on the ion dissolution rate during the final stage.

CONCLUSIONS

In this work, the dissolution behavior of a polyphosphate glass, with the composition of $45P_2O_5{\cdot}3SiO_2{\cdot}25K_2O{\cdot}15CaO{\cdot}10MgO{\cdot}ZnO{\cdot}MnO$ (mol %), in simulated body fluid (SBF) at a temperature of 37 °C for different times was studied. Two glass powder samples with different granulation, *i.e.*, from 0.1 to 0.3 and from 0.3 to 0.65 mm, as well as bulk glass samples were investigated. All experiments were conducted under static conditions. It was shown that during the glass dissolution in SBF, three stages could be distinguished. The initial stage, during the first 20 h, where the greatest changes in the dissolution rates and normalized concentrations with time were observed. The initial dissolution rates were in the range from 0.32 to 0.84 g m^{-2} h^{-1}. The diffusion coefficients were in the range from 1.90×10^{-13} to 7.7×10^{-14} m^2 h^{-1}. The second stage in the dissolution process, named the transitional stage, was in the time interval between 20 and 240 h. In this stage, changes in the normalized concentration of the ions in the solution were smaller and the dissolution rate decreased exponentially by 11 to 15 times. The last stage, named the final stage, represents dissolution times longer than 240 h. It is characterized by small linear changes in the normalized concentrations of ions and small dissolution rate changes with time, lying in the range from 8.74×10^{-4} to 7.44×10^{-3} g m^{-2} h^{-1}. The different values for the dissolution rates show that the dissolution of this glass in SBF is incongruent for the investigated times of up to 720 h.

Acknowledgment. The authors are grateful to the Ministry of Education, Science and Technological Development of the Republic of the Serbia for the financial support (Project Nos. 34001 and 172004).

ИЗВОД

РАСТВАРАЊЕ ПОЛИФОСФАТНОГ СТАКЛА У СИМУЛИРАНОЈ ТЕЛЕСНОЈ ТЕЧНОСТИ

ЈЕЛЕНА Д. НИКОЛИЋ[1], МИХАЈЛО Б. ТОШИЋ[1], СНЕЖАНА Р. ГРУЈИЋ[2], ВЛАДИМИР Д. ЖИВАНОВИЋ[1], МАРИЈА С. ЂОШИЋ[1], СРЂАН Д. МАТИЈАШЕВИЋ[1] и СОЊА В. СМИЉАНИЋ[2]

[1]Институт за технологију нуклеарних и других минералних сировина, Франше де Переа 86, 11000 Београд и [2]Универзитет у Београду, Технолошко–металуршки факултет, Карнегијева 4, 11000 Београд

У раду испитивано је понашање полифосфатног стакла састава $45P_2O_5{\cdot}3SiO_2{\cdot}25K_2O{\cdot}15CaO{\cdot}10MgO{\cdot}ZnO{\cdot}MnO$ (mol %), при растварању у симулираној телесној течности (SBF) на температури од 37 °C за различита времена. Испитане су паралелно две серије гранулација 0,1–0,3 и 0,3–0,65 mm и компактни узорци. Експерименти растварања изведени су при стационарним условима. Анализиране су временске промене нормализованих губитака масе, нормализованих концентрација јона, промене pH раствора и морфологија површине узорака. Одређене су почетне брзине растварања масе и јона, коефицијенти дифузије катјона и брзине ослобађања јона при хидролизи стакла. Резултати показују да се испитивано фосфатно стакло раствара селективно у SBF без таложења и формирања нових потенцијално токсичних једињења, за временски период растварања до 720 h.

(Примљено 31. октобра, ревидирано 5. децембра, прихваћено 6. децембра 2016)

REFERENCES

1. Z. Sheikh, S. Najeeb, Z. Khurshid, V. Verma, H. Rashid, M. Glogauer, *Materials* **8** (2015) 5744
2. A. Bandyopadhyay, S. Bernard, W. Xue, S. Bose, *J. Am. Ceram. Soc.* **89** (2006) 2675
3. O. Bretcanu, F. Baino, E. Verné, C. Vitale-Brovarone, *J. Biomater. Appl.* **28** (2014) 1287
4. E. A. A. Neel, W. Chrzanowski, D. M. Pickup, L. A. O'Dell, N. J. Mordan, R. J. Newport, M. E. Smith, J. C. Knowles, *J. R. Soc. Interface* **6** (2009) 435
5. D. S. Brauer, C. Rüssel, W. Li, S. Habelitz, *J. Biomed. Mater. Res., A* **77** (2006) 213
6. M. Navarro, M.-P. Ginebra, J. A. Planell, *J. Biomed. Mater. Res., A* **67** (2003) 1009
7. N. Vadera, A. Ashokan, G. S. Gowd, K. M. Sajesh, R. P. Chauhan, R. Jayakumar, S. V. Nair, M. Koyakutty, *Mater. Lett.* **160** (2015) 335
8. C. E. Smith, R. K. Brow, *J. Non-Cryst. Solids* **390** (2014) 51
9. E. A. A. Neel, L. A. O'Dell, W. Chrzanowski, M. E. Smith, J. C. Knowles, *J. Biomed. Mater. Res., B* **89** (2009) 392
10. M. N. Rahamana, D. E. Daya, B. S. Balb, Q. Fuc, S. B. Junga, L. F. Bonewalde, A. P. Tomasiac, *Acta Biomater*. **7** (2011) 2355
11. S. Bose, G. Fielding, S. Tarafder, A. Bandyopadhyay, *Trends Biotechnol.* **31** (2013) 594
12. E. Gentleman, Y. C. Fredholm, G. Jell, N. Lotfibakhshaiesh, M. D. O'Donnell, R. G. Hill, M. M. Stevens, *Biomaterials* **31** (2010) 3949
13. L. Wei, J. Ke, I. Prasadam, R. J. Miron, S. Lin, Y. Xiao, J. Chang, C. Wu, Y. Zhang, *Osteoporos. Int.* **25** (2014) 2089
14. T. Kokubo, H. Takadama, *Biomaterials* **27** (2006) 2907
15. A. A. Belyustin, M. M. Shultz, *Glass Phys. Chem.* **9** (1983) 3
16. G. E. Elkin, A. A. Belyustin, *Glass Phys. Chem.* **15** (1989) 285
17. S. Gin, J. P. Mestre, *J. Nucl. Mater.* **295** (2001) 83
18. A. Leidieu, F. Devreux, P. Barboux, L. Sicard, D. Spalla, *J. Non-Cryst. Solids* **356** (2010) 1458

19. T. Geisler, A. Janssen, D. Scheiter, T. Stephen, J. Berndt, A. Putnis, *J. Non-Cryst. Solids* **240** (1998) 144
20. M. B. Tošić, J. D. Nikolić, S. R. Grujić, V. D. Živanović, S. N. Zildžović, S. D. Matijašević, S. V. Ždrale, *J. Non-Cryst. Solids* **362** (2013) 185
21. M. Watanabe, *Bull. Chem. Soc. Jpn.* **47** (1974) 2048
22. M. Watanabe, M. Matsuura, T. Yamada, *Bull. Chem. Soc. Jpn.* **54** (1981) 738
23. H. Takebe, Y. Baba, H. M. Kuwabara, *J. Non-Cryst. Solids* **352** (2006) 3088
24. E. A. A. Neel, W. Chrzanowski, D. M. Pickup, L. A. O'Dell, N. J. Mordan, R. J. Newport, M. C. Smith, J. C. Knowles, *J. R. Soc. Interface* **6** (2009) 435
25. Y. M. Moustafa, K. El-Egili, *J. Non-Cryst. Solids* **240** (1998) 144
26. A. E. Efimov, *J. Non-Cryst. Solids* **209** (1997) 209
27. R. Conradt, *J. Am. Ceram. Soc*. **91** (2008) 728
28. N. Kuwata, X. Lu, T. Miyazaki, Y. Iwai, T. Tanabe, J. Kawamura, *Solid State Ionics* **294** (2016) 59
29. W. T. Tysoe, P. V. Kotvis, *Surface Chemistry of Extreme-Pressure Lubricant Additives*, in *Surface Modification and Mechanisms: Friction, Stress and Reaction Engineering*, E. Totten, H. Liang, Eds., Marcel Dekker Inc., New York, 2005, p. 350
30. P. Fugier, S. Gin, Y. Minet, T. Chave, B. Bonin, N. Godon, J. Lartigue, P. Jollivet, A. Ayral, L. Dewindt, G. Santarini, *J. Nucl. Mater*. **380** (2008) 8
31. C. Poinssot, S. Gin, *J. Nucl. Mater*. **420** (2012) 182.